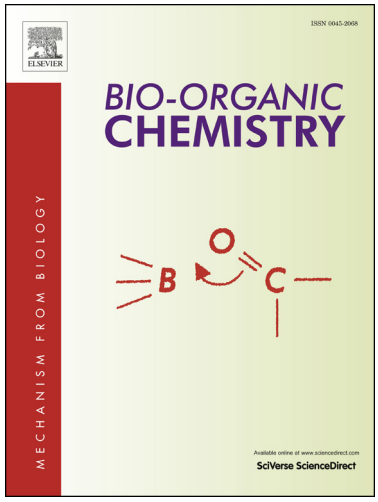

Design, synthesis, biological evaluation and molecular docking studies of novel benzofuran-pyrazole derivatives as anticancer agents

Somaia S. Abd El-Karim, Manal M. Anwar, Neama A. Mohamed, Tamer Nasr, Samia A. Elseginy

PII: S0045-2068(15)30015-8
DOI: http://dx.doi.org/10.1016/j.bioorg.2015.08.006
Reference: YBIOO 1838

To appear in: *Bioorganic Chemistry*

Received Date: 8 July 2015
Revised Date: 25 August 2015
Accepted Date: 25 August 2015

Please cite this article as: S.S. Abd El-Karim, M.M. Anwar, N.A. Mohamed, T. Nasr, S.A. Elseginy, Design, synthesis, biological evaluation and molecular docking studies of novel benzofuran-pyrazole derivatives as anticancer agents, *Bioorganic Chemistry* (2015), doi: http://dx.doi.org/10.1016/j.bioorg.2015.08.006

Design, synthesis, biological evaluation and molecular docking studies of novel benzofuran-pyrazole derivatives as anticancer agents

Somaia S. Abd El-Karim[a], Manal M. Anwar [a,*], Neama A. Mohamed[a], Tamer Nasr[b], Samia A. Elseginy[c,d]

[a]*Therapeutical Chemistry Department, National Research Centre, Dokki, Cairo, 12622, Egypt.*

[b]*Department of Pharmaceutical Chemistry, Faculty of Pharmacy, Helwan University, 11795 Helwan, Cairo, Egypt*

[c]*Green Chemistry Department, National Research Centre, Cairo, Egypt.*

[d]*School of Pharmacy and Pharmaceutical Sciences, Cardiff University, King Edward VII avenue, Cardiff, CF10 3NB, UK.*

* To corresponding author: e-mail: manal.hasan52@live.com (M.M. Anwar)

Tel.: +20 1223956970; fax: + 20 233370931.

Abstract

This study deals with design and synthesis of novel benzofuran-pyrazole hybrids as anticancer agents. Eight compounds were chosen by National Cancer Institute (NCI), USA to evaluate their *in vitro* antiproliferative activity at 10^{-5} M in full NCI 60 cell panel. The preliminary screening of the tested compounds showed promising broad-spectrum anticancer activity. Compound **4c** was further assayed for five dose molar ranges in full NCI 60 cell panel and exhibited remarkable growth inhibitory activity pattern against Leukemia CCRF-CEM, MOLT-4, Lung Cancer HOP-92, Colon Cancer HCC-2998, CNS Cancer SNB-75, Melanoma SK-MEL-2, Ovarian Cancer IGROV1, Renal Cancer 786-0, RXF 393, Breast Cancer HS 578T and T-47D (GI_{50}: 1.00 – 2.71 µM). Moreover, enzyme assays were carried out to investigate the possible antiproliferative mechanism of action of compound **4c**. The results revealed that compound **4c** has good c-Src inhibitory activity at 10 µM. In Addition, molecular docking studies showed that **4c** could bind to the ATP Src pocket sites. Fulfilling the Lipinskiís rule of five in addition to its ADME profile and the biological results, all strongly suggest that **4c** is a promising Src kinase inhibitor.

Keywords: Anticancer, Molecular docking, Benzofuran, Pyrazole

1. Introduction

Cancer still remains a potentially life threatening disease and the number of cancer related deaths are increasing alarmingly. Literature clearly indicated that more than 90% of cancer patients die due to chronic tumor metastases. Despite the presence of a large number of anticancer drugs, no currently available agents can eradicate cancer cells without harming normal tissues. Thus, the development of newer chemotherapeutic scaffolds which selectively act on the target without side effects has become a primary objective of medicinal chemists [1,2].

Literature survey revealed that substituted benzofurans could act as anticancer agents. It has been reported that phenylbenzofuran-2-carboxylic acid ethyl ester derivative (**I**) showed selective and potent cytotoxicity for human fibroblasts of lung tissues (EC_{50}; 40 ng/mL) [3]. In order to get rid of the biologically unstable ester group the 2-benzoyl-phenylbenzofuran derivative (**II**) was derived as another lead compound (EC_{50}; 600 ng/mL) [3]. Similarly, it has been reported that the 2-(2,4-dimethoxybenzoyl)-phenylbenzofuran derivative **III** was exhibiting potent cytotoxic activities against human lung carcinoma cells [4]. Moreover, Ariad Pharmaceuticals disclosed compound **IV** which carries benzofuran subunit in its structural molecule for the treatment of hyper-resorptive bone disorders through the direct inhibition of the Src protein tyrosine kinase (IC_{50} = 22 μM) [5].

Further literature survey revealed that various *N*-substituted pyrazoles have been implemented as antileukemic, antitumor, antiproliferative, anti-angiogenic, DNA interacting, proapoptotic, autophagy and antitubulin agents. In addition, these compounds are capable to exert remarkable anti-cancer effects through inhibition of different types of enzymes, proteins and receptors which play critical roles in cell division [6]. Moreover, the compound **V** bearing *N*-phenylpyrazole nucleus was developed by Vertex Pharmaceuticals as an inhibitor of Src kinases and c-Jun *N*-terminal kinases (JNKs) [5].

< Insert Fig. 1>

The non-receptor tyrosine kinase c-Src belongs to a family of closely related kinases and is widely expressed in all cell types. Over the past century, large amounts of data

have been generated supporting the role of c-Src as a key messenger in many important cellular pathways, including those involved in regulating proliferation, differentiation, survival, motility, adhesion, migration, and angiogenesis [7,8]. Because of its essential role in many intracellular signaling pathways, however, interrupting c-Src signaling may disrupt oncogenic pathways. Research has revealed that c-Src is present in a low concentration inactive form in the normal cells, while increase in its activity can be linked to increased motility/ invasiveness of tumor cells and tumor progression [9,10]. Although c-Src is rarely found as a mutated oncogene in human malignancies, elevated expression and activation of Src family kinases (SFKs) have been implicated in a variety of cancers (including glioblastoma, colon, lung, breast, and prostate cancers), osteoporosis and stroke-induced vascular permeability [11-13]. Moreover, beneficial effects of c-Src inhibition in several pathological models (cell cycle arrest of tumor cell lines, growth inhibition of Src-transformed fibroblast derived tumors, metastasis inhibition in human tumor models) has been demonstrated [14,15].

Based on the afore-mentioned findings, and in an attempt to find new potent c-Src inhibitors as anticancer agents; novel hybrid compounds having benzofuran-pyrazole backbone have been designed to evaluate their cytotoxic activity against several tumor cell lines (**Fig. 2**). This backbone was conjugated with different aromatic or heteroaromatic rings of documented potent antitumor activity such as isoxazole ring [16,17] or c-Src inhibiting activity such as pyrimidine heterocycle [18,19] in a trial to generate a new class exhibiting both enzymatic and cellular c-Src inhibition activities for maximal anti-tumor effects (**Fig. 2**). All the newly synthesized compounds were submitted to the National Cancer Institute (NCI), Bethesda, Maryland, USA, to evaluate their anticancer activity. Only eight compounds were selected by NCI and subjected to *in vitro* anticancer screening against 60 human cancer cell lines. Furthermore, the inhibitory activity was evaluated against c-Src at Kinexus Corporation. Molecular docking studies were carried out to explain how these compounds could act at the molecular level.

< Insert Fig. 2>

2. Results and Discussion

2.1. Chemistry

The synthetic pathways adopted for the preparation of the new benzofuran-pyrazole hybrid derivatives in this study is depicted in (Scheme 1). Using Vilsmeier Haach reaction, the key starting material 3-(benzofuran-2-yl)-1-phenyl-1*H*-pyrazole-4-carbaldehyde **(1)** was prepared according to the reported method [20]. It is documented that chalcones are convenient intermediates for the synthesis of five and six membered-heterocycles [21-23]. The chalcones **2a-d** were obtained in good yields by Claisen-Schmidt condensation of 3-(benzofuran-2-yl)-1-phenyl-1*H*-pyrazole-4-carbaldehyde **(1)** with various substituted ketones namely; *p*-chloroacetophenone, cyclohexylmethyl ketone, 2-acetylpyrrole and/or 2-acetylfuran in ethanolic sodium hydroxide solution. The elemental analyses and spectral data confirmed the molecular structures of the synthesized derivatives. ^{1}H-NMR spectra of the obtained derivatives displayed a pair of doublets at δ 6.31-7.10 and 7.60-8.10 ppm, with coupling constant values (*J*=15.0-15.5 Hz) due to the trans-olefinic protons. Upon treatment of the chalcone derivatives **2a-d** with hydrazine hydrate in ethanol and/or acetic acid afforded the corresponding pyrazoline and *N*-acetylpyrazoline derivatives **3a-d** and **4a-d**; respectively. The chemical structures of the obtained derivatives were established depending on the elemental and spectral data. For example, ^{1}H-NMR spectra of compounds **3a-d** exhibited, besides the expected signals of the parent protons, the two methylene protons of CH_2 of the pyrazoline ring as a pair of douplets at the regions δ 2.91-3.11 and 3.41-3.65 ppm, while its methine proton C*H* presented as two douplets at the range δ 5.19-5.26 ppm. Regarding ^{1}H-NMR spectra of **4a-d**, they represented the acetyl protons as a singlet signal at δ 2.19-2.32 ppm, the methylene protons of the pyrazoline ring as two douplets at δ 2.98-3.20 and 3.86-4.02 ppm and the methine proton as a pair of douplets at δ 5.87-5.98 ppm. Further cyclocondensation reaction of the chalcone derivatives **2a-d** with hydroxyl amine hydrochloride and thiourea was carried out to obtain the corresponding isoxazole and thiopyrimidine analogues **5a-d** and **6a-d**, respectively. The obtained derivatives were investigated on the basis of elemental analyses and spectral data. For example, their mass spectra were consistent with their chemical structures (Scheme **1**).

<Insert Scheme 1>

2.2. Pharmacology

2.2.1. Screening of anticancer activity

All the newly synthesized compounds were subjected to NCI *in vitro* anticancer screening against full 60 human cancer cell lines organized into nine sub-panels derived from nine different human cancer types: leukemia, lung, colon, CNS, melanoma, ovarian, renal, prostate and breast cancer cell lines using a single high dose concentration (10^{-5} M) under the drug discovery program of the NCI [24]. Eight compounds were selected on the basis of the degree of structure variations and computer modelling techniques for evaluation of their antineoplastic activity. The selected derivatives were **2a**, **2c**, **2d**, **3c**, **4c**, **4d**, **5d** and **6d**. The screening results of the promising compounds **2c**, **2d**, **3c**, **4c**, **4d**, **5d** were summarized in **(Table 1)**. Program generated data associated with the reference standard Staurosprorin (registered as NSC 618487) may retrieved from the DTP web site http://dtp.nci.nih.gov/dtpstandard/dwindex/index.jsp

<Insert Table 1>

The output of the single dose screening is reported as graphs of mean growth percent of the treated cells (Figures I-IV, supplementary data). This allows detecting both growth inhibition values (between 0 and 100) and cytotoxicity values (less than 0). Moreover, the results of single dose screening were analyzed by COMPARE program. Among the screened compounds, compound **4c**, benzofuran nucleus in conjugation with pyrrole-*N*-acetylpyrazoline core, exhibited significant growth inhibition against variety of cell lines. Thus, compound **4c** was further evaluated at five different minimal concentrations (0.01, 0.1, 1, 10 and 100 µM) by NCI team (**Table 2**).

Compound **4c** displayed cell growth promotion for Leukemia K-562 and SR (43.16 % and 39.11%; cell growth inhibition: 56.84% and 60.89%; respectively), Non-small cell lung cancer NCI-H322M and NCI-H460 (59.13% and 19.08%; cell growth inhibition: 40.87% and 80.92%; respectively), Colon cancer HCT-116, KM12 and SW-620 (27.86% , 58.51% and 59.18%; cell growth inhibition: 72.14%, 41.49 and 40.82%; respectively), CNS cancer SNB-75 and U251 (41.98% and 26.06%; cell growth inhibition: 58.02% and 73.94%; respectively), Melanoma LOX IMVI and MDA-MB-435 (27.31% and 49.54; cell growth inhibition: 72.69% and 50.64%; respectively), MALME-3M (cell growth promotion -2.87%; cytotoxic), Ovarian cancer OVCAR-4 and OVCAR-8 (43.55% and 55.5%; cell growth inhibition: 56.45%

and 44.50%; respectively). In addition to its cytotoxic activity against Melanoma MALME-3M, it showed cytotoxic activity against the renal cancer 786-0. Also it displayed cell growth promotion for renal A498, ACHN, CAKI-1, RXF 393, TK-10 and UO-31 in the range (26.36-65.85%) and cell growth promotion for Prostate cancer PC-3 (42.28%), and Breast cancer MCF7, MDA-MB-231/ATCC, HS 578T, T-47D in the range (45.95-55.44%).

The replacement of the pyrrole functionality of compound **4c** with furan heterocyclic ring system as compound **4d** produced the second active candidate in this study. Compound **4d** showed cell growth promotion for Leukemia MOLT-4, Melanoma SK-MEL-5, Prostate cancer PC-3, Breast cancer MCF7 and MDA-MB-468 (21.91%, 26.70%, 58.63%, 58.28% and 22.28%; cell growth inhibition: 87.09%, 73.3%, 41.37%, 41.72%, and 77.72%; respectively). Moreover, the conjugation of the bio-isosteric isoxazole ring to the furan moiety instead of the pyrazoline heterocycle as derivative **5d** retained the potency against the growth promotion of different types of the carcinoma cell lines. Compound **5d** displayed cell growth promotion for Leukemia CCRF-CEM, MOLT-4, SR (57.57%, 50.54% and 44.22%; cell growth inhibition: 42.43%, 49.46 and 55.78%; respectively). Additionally, it showed cell growth promotion for CNS cancer SNB-75 and Prostate cancer PC-3 (55.60% and 56.34%; cell growth inhibition: 44.40% and 43.66%; respectively). Moreover, compound **5d** showed cell growth promotion for Breast cancer MCF7, MDA-MB-231/ATCC and T-47D (51.64%, 55.65% and 45.72%; cell growth inhibition: 48.36%, 44.35 and 54.28%; respectively). On the other hand, the sensitivity of the tested human carcinoma cell lines apparently decreased towards the pyrrole-chalcone **2c**, the furan-chalcone **2d**. The results revealed that the pyrrole-chalcone **2c** emerged activity against Leukemia MOLT-4, SR and Breast cancer MCF7, T-47D (cell growth promotion 69.07, 67.66%, 50.02% and 55.66%, inhibition 30.93, 32.34%, 49.02 and 44.34%; respectively). The furan-chalcone **2d** displayed growth inhibition potency against Leukemia MOLT-4 (cell growth promotion 67.04%, inhibition 32.96%). Unfortunately, the tested human cell lines exhibited weak response towards the parent *p*-chlorophenyl chalcone **2a** and the pyrrolo-pyrazoline compound **3c**.

2.2.2. *In vitro* 5 dose full NCI 60 cell panel assay

Compound **4c** satisfied pre-determined threshold growth inhibition criteria and was further selected for NCI full panel five dose assay. All the sixty cell lines, representing nine tumor subpanels, were incubated at 10-fold dilutions of five

different concentrations (0.01, 0.1, 1, 10 and 100 µM). The dose response curve of nine sub-panel cell lines for compound **4c** and the reference drug Staurosprorin were represented in Figures **V, VI** (supplementary data).

The results of the tested compound were given by three response parameters (GI_{50}, TGI and LC_{50}) for each cell line from log concentration *vs* the percent growth inhibition curves on nine cancer diseases (**Table 2**). The GI_{50} value (growth inhibitory activity) corresponds to the concentration of the compound causing 50% decrease in net cell growth, the TGI value (cytostatic activity) is the concentration of the compound resulting in total growth inhibition and LC_{50} value (cytotoxic activity) is the concentration of the compound causing net 50% loss of initial cells at the end of the incubation period of 48h (**Table 2**). The mean graph midpoints (MG-MID) were also calculated for GI_{50} parameter, giving an average activity parameter over all cell panels for the tested compound **4c**.

< Insert Table 2 >

The results revealed that the compound **4c** exhibited promising growth inhibition potency against the tested tumor cell lines with average GI_{50} values (MG-MID) 2.63-7.34 µM, namely, Leukemia CCRF-CEM (GI_{50}: 1.00 µM), MOLT-4 (GI_{50}: 1.00 µM), Non-Small Cell Lung Cancer HOP-92 (GI_{50}: 2.15 µM), Colon Cancer HCC-2998 (GI_{50}: 2.71 µM), CNS Cancer SNB-75(GI_{50}: 1.79 µM), Melanoma SK-MEL-2 (GI_{50}: 2.57 µM), SK-MEL-28 (GI_{50}: 2.85 µM), SK-MEL-5 (GI_{50}: 2.80 µM), Ovarian Cancer IGROV1 (GI_{50}: 1.90 µM), Renal Cancer 786-0 (GI_{50}: 2.54 µM), RXF 393 (GI_{50}: 2.42 µM), Breast Cancer HS 578T (GI_{50}: 1.26 µM) and T-47D (GI_{50}: 2.68 µM) (**Table 2**).

2.2.3. Enzyme activity inhibition assay

Evaluation of the protein kinase inhibition activity of the most active target compounds was the main focus of this study. Thus, compound **4c** was assayed for its activity as Src protein kinase inhibitor. The assay was carried out at Kinexus Corporation, Vancouver, BC, Canada using the radio-labeled ^{33}P-ATP assay format. The assay conditions were optimized to yield acceptable enzymatic activity with high signal-to-noise ratio. The results were recorded as the percent change of the activity in comparison to the control. The intra-assay variability was determined to be less than 10%. Inhibition of the target activity by the compound gives negative value while

activation of the target activity gives positive value. Kinexus considers only values of more than 25% change in activity compared to control to be significant. The results showed that compound **4c** inhibited Src kinase at 10 µM concentration by 59 % compared to the control. The reference standard Staurosprorin inhibited Src kinase by 83 % at the same concentration. According to this promising result, it was interesting to find other protein kinase targets for the tested compound. Thus, it was assayed at 10 µM concentration against other seven protein kinases; AURORA A, BRAF, CDK2/Cyclin A2, ZAP-70, EGFR, FGFR1 and PI3Kγ. Unfortunately, only ZAP-70 was inhibited by 49 % compared to the control and the rest of the protein kinases were not significantly inhibited **(Table 3)**. The good inhibition activity of compound **4c** against Src and ZAP-70 kinases might explain its high and broad spectrum anti-proliferative potency against many NCI human cancer cell lines in which elevated expression of Src family kinases (SFKs) [10-12] and ZAP-70 [25-27] has been implicated.

< Insert Table 3 >

2.2.4. Docking studies

To further validate our rational design, compound **4c** was docked against the Kinase ATP binding site of Src kinase, using MOE (Molecular Operating Environment) 2008-10 [28]. The crystal structure of Src kinase in complex with AP23451 (co-crystalized ligand) was retrieved from the RCSB Protein Data Bank (PDB; 2BDF) and used as a target for our modelling studies. The native ligand formed H-bond with the backbone of Met341 and showed hydrophobic interaction with Leu393 and Leu273. In addition to the conserved amino acids Leu273, Val281, Ala293, Thr338, Tyr340, Leu393, Gly344 and Ser345 that surrounded the native ligand [29]. The MOE algorithm was validated by redocking the co-crystalized ligand. The result of the self-docking showed that the docked pose has the same binding mode as the native ligand and occupies the same surface area of Src pocket site (**Fig. 3**). This result indicates the reliability of MOE algorithm with 2BDF complex.

< Insert Figure 3 >

The docking results of compound **4c** exhibited interesting interactions between compound **4c** and the receptor. It can be identified as following: (i) the NH of the

pyrrole ring formed H-bond with Lys343 (2.78Å) and the nitrogen atom of pyrazoline moiety formed H-bond with Ser345 (3.24Å); one of the conserved amino acids (ii) the phenyl group of benzofuran moiety was surrounded by Tyr340, Met341 and Ser342 and the pyrazole ring represented closure to Asp348 that might suggest hydrophobic interactions. The phenyl group of compound **4c** showed hydrophobic interaction with Leu273 and Gly274 (**Fig. 4**). Moreover, compound **4c** showed good fitting within ATP Src binding site similar to the native ligand (**Fig. 5**). The good fitting and interactions of **4c** within Src kinase binding site correlate with the enzymatic assay results.

< Insert Figure 4>

< Insert Figure 5>

Lipinskiís rule of five and ADME profile

We assessed compound **4c** using ADME (adsorption, distribution, metabolism, elimination) method. In particular, we investigated the consistent of compound **4c** to the Lipinskiís rule of five [30]. Briefly, this simple rule is based on the observation that most orally administered drugs have a molecular weight (MW) of 500 or less, five or fewer hydrogen bond donor sites and 10 or fewer hydrogen bond acceptor sites. In addition, we calculated the polar surface area (PSA), since it is another key property that has been linked to the drug bioavailability. Thus, passively absorbed molecules with a PSA >140 Å are thought to have low oral bioavailability [31]. Our results showed that compound **4c** fulfilled Lipinski rule (MW = 435.48, one hydrogen bond acceptor and one hydrogen bond donor) (**Table 4**). In addition, it also fulfilled the topological descriptors and fingerprints of molecular drug-likeness structure keys as LogP and Log S.

< Insert Table 4 >

2.2.5. Structure activity relationship (SAR)

The results of the anticancer screening demonstrated the following assumptions about the structure activity relationship (SAR) (**Fig. 6**):

< Insert Figure 6 >

- The combination of 3-pyrrolo-*N*-acetylpyrazoline or 3-furano-*N*-acetylpyrazoline conjugates with the basic benzofuran-*N*-phenylpyrazole core as compound **4c** and **4d** exhibited the most potent anti-proliferative activity.
- The attachment of the electron withdrawing acetyl group to *N*-1 of pyrazoline ring appeared to be essential for potent cancerous inhibitory effect, since the pyrrolo-pyrazoline candidate **3c** represented weak anti-proliferative activity against most of the tested human cancer cell lines.
- Furthermore, the same high anti-proliferative potency was gained upon replacement of the *N*-acetylpyrazoline moiety with the bioisostere isoxazole ring but retaining the furan heterocycle as compound **5d**.
- Apparent decrease in the potency was noticed by the parent chalcones even in the presence of the pyrrole and furan rings as the derivatives **2a**, **2c** and **2d**.
- The increase in the size of the hetero-ring systems attached to the parent core as thiopyrimidine rings resulted in weak to moderate anti-proliferative potency.
- It can be concluded that the highest activity that was obtained by compounds **4c**, **4d**, **5d** could be attributed to the synergistic effects of the parent benzofuran-*N*-phenylpyrazole skeleton together with the 3-pyrrolo/furano-*N*-acetylpyrazoline or 3-pyrrolo-isoxazole ring systems.

3. Conclusion

In this study, novel benzofuran-pyrazole hybrid derivatives were successfully synthesized and eight of them were selected by NCI, USA to evaluate their *in vitro* anticancer activities against full 60 human cancer cell lines at a single high dose (10^{-5} M) concentration. The hybrids clubbed with 3-furano-*N*-acetylpyrazoline and 3-furano-isoxazole rings **4d**, **5d** produced remarkable and broad spectrum anticancer activities. The most potent activity was obtained by the derivative bearing 3-pyrrolo-*N*-acetylpyrazoline **4c** which was further selected and evaluated by NCI against full panel of cell lines at five different minimal concentrations. Enzyme assay study revealed that compound **4c** is a good inhibitor of Src and ZAP-70 kinases. Fulfilling the Lipinskiís rule of five together with its ADME profile and the anticancer results

all revealed that compound **4c** is a promising scaffold for further modification of more potent and selective anticancer agents.

4. Experimental

4.1. Chemistry

All melting points are uncorrected and were taken in open capillary tubes using Electrothermal apparatus 9100. Elemental microanalyses were carried out at Microanalytical Unit, Central Services Laboratory, National Research Centre, Dokki, Cairo, Egypt, using Vario Elementar and were found within ±0.4% of the theoretical values. Infrared spectra were recorded on FT/IR-4100 Jasco-Japan, Fourier transform, Infrared spectrometer at cm^{-1} scale using KBr disc technique at Central Services Laboratory, National Research Centre, Dokki, Cairo, Egypt. ^{1}H-NMR and ^{13}C-NMR spectra were determined by using a JEOL AS-500 NMR spectrometer at Central Services Laboratory, National Research Centre, Dokki, Cairo, Egypt, chemical shifts are expressed in δ (ppm) downfield from TMS as an internal standard. The mass spectra were measured with a GC MS-Qp1000EX Shimadzu, Cairo University, Cairo, Egypt and Finnigan MAT SSQ-7000 mass spectrometer at Central Services Laboratory, National Research Centre, Dokki, Cairo, Egypt. Follow up of the reactions and checking the purity of the compounds were made by TLC on silica gel-precoated aluminium sheets (Type 60, F 254, Merck, Darmstadt, Germany) using chloroform/methanol (20:1, v/v) and the spots were detected by exposure to UV lamp at λ_{254} nanometer for few seconds and by iodine vapor. The chemical names given for the prepared compounds are according to the IUPAC system. 3-(benzofuran-2-yl)-1-phenyl-1*H*-pyrazole-4-carbaldehyde (**1**) was prepared according the reported method [20].

4.1.1. 3-(3-(Benzofuran-2-yl)-1-phenyl-1H-pyrazol-4-yl)-1-(substituted)prop-2-en-1-one 2a-d

A mixture of carbaldehyde **1** (2.88 g, 0.01 mol) and the appropriate acetyl derivatives namely; 4-chloroacetophenone, cyclohexylmethyl ketone, 2-acetylpyrrole and/or 2-acetylfuran (0.01 mol) in alcoholic sodium hydroxide solution (30 mL, 10%) was stirred for 3h. The reaction mixture was left overnight at room temperature. The formed precipitate was filtered, washed several times with water, dried and recrystallized from ethanol to give the target compounds **2a-d** respectively.

4.1.1.1. 3-(3-(Benzofuran-2-yl)-1-phenyl-1H-pyrazol-4-yl)-1-(4-chlorophenyl)prop-2-en-1-one (2a)

Yield 90%, mp. 154-156^{o}C, pale yellow; IR (KBr, cm^{-1}): 3062 (CH-arom.), 1676 (C=O); ^{1}H NMR (DMSO-d$_6$): δ 7.10 (1H, d, *J* = 15.0 Hz, CH=) 7.22-7.61 (14H, m, Ar-H), 7.79 (1H, *J* = 15.0 Hz, CH=), 8.71 (1H, s, pyrazole-H$_5$); ^{13}C NMR (DMSO-d$_6$): δ 198.18 (CO), 104.28, 105.94, 111.81, 118.63, 118.95, 119.43, 122.23, 122.46, 125.83, 128.20, 129.24, 129.51, 130.16, 130.37, 130.71, 134.72, 135.70, 138.66, 143, 80, 150.00, 150.48 (arom. C); MS, m/z (%): 424, 426 [M^{+}] (15, 10), 423, 425 [M^{+}-1] (13, 7), 285 [M^{+} -C$_7$H$_4$ClO] (100); Anal. For C$_{26}$H$_{17}$ClN$_2$O$_2$ (424.88): Calcd. C, 73.50; H, 4.03; N, 6.59; Found: C, 73.23; H, 4.15; N, 6.36.

4.1.1.2. 3-(3-(Benzofuran-2-yl)-1-phenyl-1H-pyrazol-4-yl)-1-cyclohexylprop-2-en-1-one (2b)

Yield 87%, mp. 176-178^{o}C, yellow powder; IR (KBr, cm^{-1}): 3063 (CH-arom.), 2920, 2851 (CH-aliph.), 1640 (C=O); ^{1}H NMR (DMSO-d$_6$): δ 1.31, 1.66, 1.77, 1.90 (10H, m, 5(CH$_2$)-cyclohexyl protons), 2.69 (1H, m, CH-cyclohexyl proton), 7.02 (1H, d, *J* = 15.2 Hz, CH=), 7.30-7.86 (10H, Ar-H), 7.97 (1H, d, *J* = 15.2 Hz, CH=), 9.33 (1H, s, pyrazole-H$_5$); ^{13}C NMR (DMSO-d$_6$): δ 25.76, 26.11, 28.78, 48.95 (cyclohexyl C), 202.34 (CO), 105.73, 111.77, 118.71, 119.35, 122.17, 124.04, 125.52, 125.78, 128.02, 128.49, 129.14, 130.27, 131.83, 139.28, 143.46, 149.76, 154.83 (arom. C); MS, m/z (%): 396 [M^{+}] (5), 313 [M^{+}-C$_6$H$_{11}$] (30), 285 [M^{+}-C$_7$H$_{11}$O] (26), 77 [C$_6$H$_5$] (100); Anal. For C$_{26}$H$_{24}$N$_2$O$_2$ (396.48): Calcd. C, 78.76; H, 6.10; N, 7.07; Found: C, 78.84; H, 5.91; N, 7.24.

4.1.1.3. 3-(3-(Benzofuran-2-yl)-1-phenyl-1H-pyrazol-4-yl)-1-(1H-pyrrol-2-yl)prop-2-en-1-one (2c)

Yield 88%, mp. 212-214^{o}C, yellow powder; IR (KBr, cm^{-1}): 3237 (NH), 3044 (CH-arom.), 1645 (CO); ^{1}H NMR (DMSO-d$_6$): 6.31 (1H, d, *J* = 15.0 Hz, CH=), 7.25-8.10 (14H, m, Ar-H, CH=, pyrrole protons), 9.40 (1H, s, pyrazole-H$_5$), 11.95 (1H, s, NH, D$_2$O exchangeable); ^{13}C NMR (DMSO-d$_6$): δ 178.20 (CO), 105.73, 110.65, 111.79, 117.44, 119.36, 122.14, 124.00, 124.37, 125.66, 126.95, 127.96, 128.54, 129.00, 130.24, 130.56, 133.64, 139.35, 143.38, 149.85, 154.85 (arom. C); MS, m/z (%): 379 [M^{+}] (17), 380 [M^{+}+1] (6), 285 [M^{+}-C$_5$H$_3$NO] (100); Anal. For C$_{24}$H$_{17}$N$_3$O$_2$ (379.41): Calcd. C, 75.97; H, 4.52; N, 11.08; Found: C, 75.71; H, 4.88; N, 11.26.

4.1.1.4. 3-(3-(Benzofuran-2-yl)-1-phenyl-1H-pyrazol-4-yl)-1-(furan-2-yl)prop-2-en-1-one (2d)

Yield 92%, mp. 144-145^{o}C, yellow powder; IR (KBr, cm^{-1}): 3060 (CH-arom.), 1653 (CO); ^{1}H NMR (DMSO-d$_6$): δ 6.67 (1H, d, *J* = 15.5 Hz, CH=), 7.25-8.10 (14H, m, Ar-H, CH=, furan protons), 8.69 (1H, s, pyrazole-H$_5$); ^{13}C NMR (DMSO-d$_6$): δ 186.50 (CO), 103.60, 103.96, 110.90, 112.25, 112.63, 117.66, 118.56, 124.45, 125.04, 126.88, 128.01, 128.18, 129.47, 139.14, 141.44, 147.22, 148.28, 149.90, 151.94, 151.97, 153.83 (arom. C); MS, m/z (%): 380 [M^{+}] (13), 381 [M^{+}+1] (9), 285 [M^{+}-C$_5$H$_3$O$_2$] (49), 95 [C$_5$H$_3$O$_2$] (100); Anal. For C$_{24}$H$_{16}$N$_2$O$_3$ (380.40): Calcd. C, 75.78; H, 4.24; N, 7.36; Found: C, 75.51; H, 4.50; N, 7.15.

4.1.2. 3-(Benzofuran-2-yl)-4-(3-substituted-4,5-dihydro-1H-pyrazol-5-yl)-1-phenyl-1H-pyrazole 3a-d

A mixture of chalcones **2a-d** (0.002 mol) and hydrazine hydrate (0.2 mL, 98%) in absolute ethanol was refluxed for 3h. The formed precipitate during heating was filtered, dried and recrystallized from absolute ethanol to give the compounds **3a-d** respectively.

4.1.2.1. 3-(Benzofuran-2-yl)-4-(3-(4-chlorophenyl)-4,5-dihydro-1H-pyrazol-5-yl)-1-phenyl-1H-pyrazole (3a)

Yield 56%, mp. 197-199^{o}C, yellow powder; IR (KBr, cm^{-1}): 3233 (NH), 3069 (CH-arom.), 2969, 2888 (CH-aliph.); ^{1}H NMR (DMSO-d$_6$): δ 3.02-3.11 (1H, dd, *J* = 11.0, 5.7 Hz, pyrazoline-H$_4$), 3.56-3.65 (1H, dd, *J* = 11.1, 6.8 Hz,pyrazoline-H$_{4'}$), 5.25-5.31 (1H, dd, *J* = 12.0, 5.8 Hz, pyrazoline-H$_5$), 5.78 (1H, br.s, NH, D$_2$O exchangeable), 7.09-7.94 (14H, m, Ar-H), 8.62 (1H, s, pyrazole-H$_5$); ^{13}C NMR (DMSO-d$_6$): δ 50.04 (pyrazolinyl C-4), 55.70 (pyrazolinyl C-5), 104.83, 111.84, 118.92, 121.84, 123.83, 124.50, 125.28, 127.23, 127.74, 127.84, 128.83, 129.07, 130.17, 132.55, 133.05, 139.71, 141.90, 148.91, 150.08, 154.57 (arom. C); MS, m/z (%): 438, 440 [M^{+}] (14, 5), 77 [C$_6$H$_5$] (100); Anal. For C$_{26}$H$_{19}$ClN$_4$O (438.91): Calcd. C, 71.15; H, 4.36; N, 12.77; Found: C, 71.32; H, 4.49; N, 12.53.

4.1.2.2. 3-(Benzofuran-2-yl)-4-(3-cyclohexyl-4,5-dihydro-1H-pyrazol-5-yl)-1-phenyl-1H-pyrazole (3b)

Yield 98%, mp. 135-137^{o}C, yellow powder; IR (KBr, cm^{-1}): 3128 (NH), 3060 (CH-arom.), 2925, 2852 (CH-aliph.); ^{1}H NMR (DMSO-d$_6$): δ 1.36, 1.70, 1.86 (10H, m, 5(CH$_2$)-cyclohexyl protons), 2.63 (1H, m, CH-cyclohexyl proton), 2.96-3.10 (1H, dd,

J = 11.4, 5.1 Hz, pyrazoline-H_4), 3.41-3.49 (1H, dd, *J* = 11.3, 6.1 Hz,pyrazoline-$H_{4'}$), 5.15-5.21 (1H, dd, *J* = 11.0, 5.6 Hz, pyrazoline-H_5), 7.18-7.99 (10H, m, Ar-H), 8.63 (1H, s, pyrazole-H_5), 10.25 (1H, br.s, NH, D_2O exchangeable); ^{13}C NMR (DMSO-d_6): δ 25.64, 26.07, 30.70, 32.96, 48.97 (cyclohexyl C), 50.57 (pyrazolinyl C-4), 54.75 (pyrazolinyl C-5), 101.82, 104.84, 111.71, 118.85, 118.98, 121.80, 123.76, 127.12, 128.81, 130.16, 139.64, 139.75, 150.17, 154.53 (arom. C); MS, m/z (%): 410 [M^+] (7), 77 [C_6H_5] (100); Anal. For $C_{26}H_{26}N_4O$ (410.51): Calcd. C, 76.07; H, 6.38; N, 13.65; Found: C, 76.34; H, 6.45; N, 13.84.

4.1.2.3. 3-(Benzofuran-2-yl)-4-(4,5-dihydro-3-(1H-pyrrol-2-yl)-1H-pyrazol-5-yl)-1-phenyl-1H-pyrazole (3c)

Yield 60%, mp. 204-205°C, white powder; IR (KBr, cm^{-1}): 3282, 3212 (2NH), 3056 (CH-arom.), 2960, 2856 (CH-aliph.); ^{1}H NMR (DMSO-d_6): δ 2.91-3.00 (1H, dd, *J* = 11.2, 5.0 Hz, pyrazoline-H_4), 3.47-3.52 (1H, dd, *J* = 11.7, 5.9 Hz, pyrazoline-$H_{4'}$), 5.12-5.16 (1H, dd, *J* = 12.0, 5.8 Hz, pyrazoline H_5), 6.07 (1H, d, *J* = 6.71 Hz, pyrrole-H_3), 6.28 (1H, m, pyrrole proton), 6.80 (1H, d, *J* = 6.70 Hz, pyrrole-H_5), 7.14-7.93 (10H, m, Ar-H), 8.58 (1H, s, pyrazole-H_5), 10.18, 11.19 (2H, 2br.s, 2NH, D_2O exchangeable); ^{13}C NMR (DMSO-d_6): δ 54.04 (pyrazolinyl C-4), 54.79 (pyrazolinyl C-5), 104.33, 108.12, 108.84, 109.20, 111.00, 117.99, 118.68, 120.02, 121.00, 121.48, 123.13, 124.65, 125.63, 126.87, 127.50, 128.27, 129.51, 139.18, 141.37, 144.77, 149.63, 154.00 (arom. C); MS, m/z (%): 393 [M^+] (85), 392 [M^+-1] (39), 77 [C_6H_5] (100); Anal. For $C_{24}H_{19}N_5O$ (393.44): Calcd. C, 73.27; H, 4.87; N, 17.80; Found: C, 73.55; H, 4.59; N, 17.62.

4.1.2.4. 3-(Benzofuran-2-yl)-4-(3-(furan-2-yl)-4,5-dihydro-1H-pyrazol-5-yl)-1-phenyl-1H-pyrazole (3d)

Yield 52%, mp. 182-183°C, yellow powder; IR (KBr, cm^{-1}): 3229 (NH), 3049 (CH-arom.), 2934, 2850 (CH-aliph.); ^{1}H NMR (DMSO-d_6): δ 2.95-3.03 (1H, dd, *J* = 11.3, 6.1 Hz, pyrazoline-H_4), 3.51-3.57 (1H, dd, *J* = 11.7, 5.8 Hz, pyrazoline-H4′), 5.19-5.26 (1H, dd, *J* = 11.9, 6.1 Hz, pyrazoline-H_5), 6.56, 6.66 (2H, d, d, *J* = 6.8 Hz, furan-$H_{3,5}$), 7.33-8.00 (11H, m, Ar-H, furan-H_4), 8.59 (1H, s, pyrazole-H_5), 10.20 (1H, br.s, NH, D_2O exchangeable); ^{13}C NMR (DMSO-d_6): δ 53.10 (pyrazolinyl C-4), 55.27 (pyrazolinyl C-5), 104.81, 109.86, 111.86, 112.20, 118.92, 121.85, 123.84, 124.35, 125.29, 127.22, 127.84, 130.17, 139.72, 141.86, 142.18, 144.01, 148.92, 150.09, 154.57 (arom. C); MS, m/z (%): 394 [M^+] (27), 393 [M^+-1] (16), 51 [C_4H_3] (100);

Anal. For $C_{24}H_{18}N_4O_2$ (394.43): Calcd. C, 73.08; H, 4.60; N, 14.20; Found: C, 73.31; H, 4.75; N, 14.43.

4.1.3. 1-(5-(3-(Benzofuran-2-yl)-1-phenyl-1H-pyrazol-4-yl)-3-substituted-4,5-dihydropyrazol-1-yl)ethanone 4a-d

A mixture of chalcones **2a-d** (0.002 mol) and hydrazine hydrate (0.2 mL, 98%) in glacial acetic acid (15 mL) was refluxed for 3h. The formed precipitate during heating was filtered, dried and recrystallized from acetic acid to give the target compounds **4a-d** respectively.

4.1.3.1. 1-(5-(3-(Benzofuran-2-yl)-1-phenyl-1H-pyrazol-4-yl)-3-(4-chlorophenyl)-4,5-dihydropyrazol-1-yl)ethanone (4a)

Yield 64%, mp. 160-162^{o}C, creamy powder; IR (KBr, cm^{-1}): 3057 (CH-arom.), 2923, 2853 (CH-aliph.), 1662 (C=O); ^{1}H NMR (DMSO-d$_6$): δ 2.23 (3H, s, $COCH_3$), 3.09-3.16 (1H, m, pyrazoline-H_4), 3.98-4.08 (1H, m, pyrazoline-$H_{4'}$), 5.94-5.98 (1H, m, pyrazoline-H_5), 7.18-7.98 (14H, m, Ar-H), 8.51 (1H, s, pyrazole-H_5); ^{13}C NMR (DMSO-d$_6$): δ; 21.26 (CO*CH$_3$*), 42.18 (pyrazolinyl C-4), 52.22 (pyrazolinyl C-5), 168.53 (*CO*CH$_3$), 104.28, 111.77, 118.92, 121.86, 123.87, 124.14, 125.28, 127.26, 128.92, 129.31, 130.07, 135.06, 139.57, 142.34, 150.51, 153.99 (arom. C); MS, m/z (%): 480, 482 [M$^+$] (13, 5), 437 [M$^+$-$COCH_3$] (8), 77 [C_6H_5] (100); Anal. For $C_{28}H_{21}ClN_4O_2$ (480.94): Calcd. C, 69.92; H, 4.40; N, 11.65; Found: C, 70.12; H, 4.68; N, 11.46.

4.1.3.2. 1-(5-(3-(Benzofuran-2-yl)-1-phenyl-1H-pyrazol-4-yl)-3-cyclohexyl-4,5-dihydropyrazol-1-yl)ethanone (4b)

Yield 61%, mp. 127-129^{o}C, creamy powder; IR (KBr, cm^{-1}): 3060 (CH-arom.), 2925, 2851 (CH-aliph.), 1658 (CO); ^{1}H NMR (DMSO-d$_6$): δ 1.35, 1.64, 1.79 (10H, m, 5(CH_2)-cyclohexyl protons), 2.19 (3H, s, $COCH_3$), 2.62 (1H, m, CH-cyclohexyl proton), 2.98-3.12 (1H, m, pyrazoline-H_4), 3.86-4.01 (1H, m, pyrazoline-$H_{4'}$), 5.87-5.92 (1H, m, pyrazoline-H_5), 7.13-7.94 (10H, m, Ar-H), 8.66 (1H, s, pyrazole-H_5); ^{13}C NMR (DMSO-d$_6$): δ; 21.54 (CO*CH$_3$*), 21.96, 25.25, 29.74 (cyclohexyl C), 42.48 (pyrazolinyl C-4), 50.90 (pyrazolinyl C-5), 167.23 (*CO*CH$_3$), 104.01, 104.19, 111.08, 118.12, 118.62, 121.39, 123.19, 124.00, 124.70, 126.11, 126.66, 128.19, 129.49, 139.03, 140.22, 149.42, 154.02, 162.64 (arom. C); MS, m/z (%): 452 [M$^+$] (10), 453 [M$^+$+1] (5), 409 [M$^+$-$COCH_3$] (5), 77 [C_6H_5] (100); Anal. For $C_{28}H_{28}N_4O_2$ (452.55): Calcd. C, 74.31; H, 6.24; N, 12.38; Found: C, 74.42; H, 6.43; N, 12.16.

4.1.3.3. 1-(5-(3-(Benzofuran-2-yl)-1-phenyl-1H-pyrazol-4-yl)-4,5-dihydro-3-(1H-pyrrol-2-yl)pyrazol-1-yl)ethanone (4c)

Yield 66%, mp. 140-142^{o}C, grey powder; IR (KBr, cm^{-1}): 3222 (NH), 3040 (CH-arom.), 2933, 2852 (CH-aliph.), 1698 (C=O); ^{1}H NMR (DMSO-d$_6$): δ 2.32 (3H, s, $COCH_3$), 3.13-3.20 (1H, dd, *J* = 11.2, 5.7 Hz, pyrazoline-H_4), 3.88-3.98 (1H, dd, *J* = 11.7, 5.8 Hz, pyrazoline-$H_{4'}$), 5.87-5.92 (1H, dd, *J* = 12.0, 5.6 Hz, pyrazoline-H_5), 6.13, 6.95 (2H, d, d, *J* =7.0 Hz, pyrrole-$H_{3,5}$), 6.52 (1H, m, pyrrole-H_4), 7.27-8.35 (10H, m, Ar-H), 9.62 (1H, s, pyrazole-H_5), 11.43 (1H, br.s, NH, D_2O exchangeable); ^{13}C NMR (DMSO-d$_6$): δ 22.38 (CO*CH$_3$*), 42.50 (pyrazolinyl C-4), 51.69 (pyrazolinyl C-5), 168.59 (*CO*CH_3), 104.58, 109.80, 111.72, 111.84, 112.78, 118.97, 121.86, 122.81, 122.93, 123.89, 124.16, 124.34, 125.29, 127.27, 128.78, 130.07, 139.58, 140.85, 148.75, 150.03, 154.59, 167.70 (arom. C); MS, m/z (%): 434 [M^+-1] (14), 433 [M^+-2] (12), 93 [C_6H_7N] (100); Anal. For $C_{26}H_{21}N_5O_2$ (435.48): Calcd. C, 71.71; H, 4.86; N, 16.08; Found: C, 71.52; H, 4.61; N, 16.36.

4.1.3.4. 1-(5-(3-(Benzofuran-2-yl)-1-phenyl-1H-pyrazol-4-yl)-3-(furan-2-yl)-4,5-dihydropyrazol-1-yl)ethanone (4d)

Yield 57%, mp. 149-150^{o}C, pale brown powder; IR (KBr, cm^{-1}): 3062 (CH-arom.), 2925, 2849 (CH-aliph.), 1659 (CO); ^{1}H NMR (DMSO-d$_6$): δ ^{1}H NMR (DMSO-d$_6$): δ 2.31 (3H, s, $COCH_3$), 3.04-3.12 (1H, m, pyrazoline-H_4), 3.92-4.02 (1H, m, pyrazoline- $H_{4'}$), 5.91-5.95 (1H, m, pyrazoline H_5), 6.63, 6.97 (2H, d, d, *J* =6.9 Hz, furan-$H_{3,5}$), 7.29-7.93 (11H, m, Ar-H, furan-H_4), 8.42 (1H, s, pyrazole-H_5); ^{13}C NMR (DMSO-d$_6$): δ 22.50 (CO*CH$_3$*), 42.75 (pyrazolinyl C-4), 52.00 (pyrazolinyl C-5), 168.21 (*CO*CH_3), 104.56, 111.79, 112.72, 118.79, 118.94, 121.87, 123.91, 123.98, 125.32, 127.24, 128.76, 130.06, 139.57, 141.00, 146.04, 146.23, 150.00, 154.59 (arom. C); MS, m/z (%): 436 [M^+] (47), 435 [M^+-1] (34), 393 [M^+-$COCH_3$] (36), 60 [C_3H_8O] (100); Anal. For $C_{26}H_{20}N_4O_3$ (436.46): Calcd. C, 71.55; H, 4.62; N, 12.84; Found: C, 71.31; H, 4.44; N, 12.97.

4.1.4. 3-(Benzofuran-2-yl)-4-(3-substituted)isoxazol-5-yl)-1-phenyl-1H-pyrazole 5a-d

A mixture of chalcones **2a-d** (0.002 mol) and hydroxyl amine hydrochloride (0.14 g, 0.002 mol) in ethanolic sodium hydroxide solution (15 mL, 5%) was refluxed for 10h. After cooling, the formed precipitate was filtered, washed several times with water,

dried and recrystallized from absolute ethanol to give the compounds **5a-d** respectively.

4.1.4.1. 3-(Benzofuran-2-yl)-4-(3-(4-chlorophenyl)isoxazol-5-yl)-1-phenyl-1H-pyrazole (5a)

Yield 90%, mp. 160-162^{o}C, pale yellow powder; IR (KBr, cm^{-1}): 3063 (CH-arom.); ^{1}H NMR (DMSO-d$_6$): δ 7.11-8.02 (15H, m, Ar-H, isoxazole-H$_4$), 8.59 (1H, s, pyrazole-H$_5$); ^{13}C NMR (DMSO-d$_6$): δ 103.66, 104.77, 111.36, 111.61, 118.82, 121.27, 123.68, 124.51, 125.04, 127.05, 127.22, 127.81, 128.53, 129.13, 130.10, 133.64, 135.31, 139.50, 142.51, 143.13, 150.21, 154.33, 155.21 (arom. C); MS, m/z (%): 437, 439 [M^{+}] (3, 6), 438, 440 [M^{+}+1] (5, 2), 77 [C$_6$H$_5$] (100); Anal. For $C_{26}H_{16}ClN_3O_2$ (437.88): Calcd. C, 71.32; H, 3.68; N, 9.60; Found: C, 71.51; H, 3.35; N, 9.49.

4.1.4.2. 3-(Benzofuran-2-yl)-4-(3-cyclohexylisoxazol-5-yl)-1-phenyl-1H-pyrazole (5b)

Yield 97%, mp. 221-223^{o}C, pale yellow powder; IR (KBr, cm^{-1}): 3057 (CH-arom.), 2922, 2849 (CH-aliph.); ^{1}H NMR (DMSO-d$_6$): δ 1.39-1.42, 1.76-1.81, 1.95, 2.70 (11H, m, cyclohexyl protons), 7.30-8.02 (10H, m, Ar-H, isoxazole-H$_4$), 9.17 (1H, s, pyrazole-H$_5$); ^{13}C NMR (DMSO-d$_6$): δ 26.62, 26.81, 32.16 (cyclohexyl C), 104.86, 111.47, 117.79, 119.19, 120.65, 122.02, 123.74, 123.97, 125.52, 127.27, 127.56, 128.55, 130.10, 139.49, 142.43, 150.42, 154.71, 157.59 (arom. C); MS, m/z (%): 411 [M^{+}+2] (61), 326 [M^{+}-C$_6$H$_{11}$] (8), 77 [C$_6$H$_5$] (100); Anal. For $C_{26}H_{23}N_3O_2$ (409.48): Calcd. C, 76.26; H, 5.66; N, 10.26; Found: C, 76.41; H, 5.42; N, 10.43.

4.1.4.3. 4-(3-(1H-pyrrol-2-yl)isoxazol-5-yl)-3-(benzofuran-2-yl)-1-phenyl-1H-pyrazole (5c)

Yield 61%, mp. 220-222^{o}C, brown powder; IR (KBr, cm^{-1}): 3234 (NH), 3057 (CH-arom.); ^{1}H NMR (DMSO-d$_6$): δ 6.30 (1H, d, pyrrole proton), 7.19-8.03 (13H, m, Ar-H, isoxazole-H$_4$, pyrrole protons), 9.40 (1H, s, pyrazole-H$_5$), 11.98 (1H, s, NH, D$_2$O exchangeable); ^{13}C NMR (DMSO-d$_6$): δ 104.35, 106.88, 111.31, 117.53, 120.22, 121.54, 122.34, 123.51, 123.94, 125.08, 126.98, 127.38, 128.41, 129.13, 131.02, 138.89, 141.71, 151.08, 154, 61, 158.82 (arom. C); MS, m/z (%): 392 [M^{+}] (62), 326 [M^{+}-C$_4$H$_4$N] (67), 92 [C$_6$H$_6$N] (100); Anal. For $C_{24}H_{16}N_4O_2$ (392.41): Calcd. C, 73.46; H, 4.11; N, 14.28; Found: C, 73.30; H, 4.25; N, 14.09.

4.1.4.4. 3-(Benzofuran-2-yl)-4-(3-(furan-2-yl)isoxazol-5-yl)-1-phenyl-1H-pyrazole (5d)

Yield 79%, mp. 119-121^{o}C, white powder; IR (KBr, cm^{-1}): 3060 (CH-arom.); ^{1}H NMR (DMSO-d$_6$): δ 6.50, 6.72 (2H, d, d, *J* = 6.8 Hz, furan-H$_{3,5}$), 7.18-7.96 (12H, m, Ar-H, furan-H$_4$, isoxazole-H$_4$), 8.67 (1H, s, pyrazole-H$_5$); ^{13}C NMR (DMSO-d$_6$): δ 105.21, 106.02, 111.87, 120.95, 121.07, 121.89, 122.48, 122.86, 123.56, 125.41, 126.28, 127.04, 127.92, 128.71, 130.58, 139.04, 140.64, 150.83, 155, 23, 159.03 (arom. C); MS, m/z (%): 393 [M^{+}] (26), 394 [M^{+}+1] (9), 77 [C$_6$H$_5$] (100); Anal. For $C_{24}H_{15}N_3O_3$ (393.39): Calcd. C, 73.27; H, 3.84; N, 10.68; Found: C, 73.56; H, 3.61; N, 10.42.

4.1.5. 6-(3-(Benzofuran-2-yl)-1-phenyl-1H-pyrazol-4-yl)-4- substituted-pyrimidine-2(1H)-thione 6a-d

A mixture of chalcones **2a-d** (0.002 mol) and thiourea (0.16 g, 0.002 mol) in ethanolic potassium hydroxide solution (15 mL, 5%) was refluxed for 24h. The reaction mixture was poured onto ice/cold water acidified by hydrochloric acid. The formed precipitate was filtered, washed several times with water, dried and recrystallized from absolute ethanol to give the title compounds **6a-d** respectively.

4.1.5.1. 6-(3-(Benzofuran-2-yl)-1-phenyl-1H-pyrazol-4-yl)-4-(4-chlorophenyl)pyrimidine-2(1H)-thione (6a)

Yield 69%, mp. 148-150^{o}C, yellowsh brown powder; IR (KBr, cm^{-1}): 3125 (NH), 3057 (CH-arom.), 1252 (CS); ^{1}H NMR (DMSO-d$_6$): δ 5.44 (1H, s, pyrimidine-H$_5$), 7.18-8.04 (14H, m, Ar-H), 8.57 (1H, s, pyrazole-H$_5$), 9.38 (1H, s, NH, D$_2$O exchangeable); ^{13}C NMR (DMSO-d$_6$): δ 96.84 (pyrimidinyl C5), 177.24 (CS), 104.21, 111.51, 118.35, 121.84, 122.59, 123.60, 124.96, 125.49, 127.04, 127.82, 128.83, 129.37, 131.05, 132.46, 133.12, 140.58, 141.86, 148.72, 151.22, 155.63 (arom. C); MS, m/z (%): 479, 481 [M^{+}-1] (7, 2), 436, 438 [M^{+}-CS] (3, 8), 77 [C$_6$H$_5$] (100); Anal. For $C_{27}H_{17}ClN_4OS$ (480.97): Calcd. C, 67.42; H, 3.56; N, 11.65; S, 6.67; Found: C, 67.28; H, 3.71; N, 11.43; S, 6.40.

4.1.5.2. 6-(3-(Benzofuran-2-yl)-1-phenyl-1H-pyrazol-4-yl)-4-cyclohexylpyrimidine-2(1H)-thione (6b)

Yield 88%, mp. 228-230^{o}C, pale yellow powder; IR (KBr, cm^{-1}): 3191 (NH), 3078 (CH-arom.), 2924, 2851 (CH-aliph.), 1281 (C=S); ^{1}H NMR (DMSO-d$_6$): δ 1.06-1.18, 1.35, 1.60-1.65, 1.96-2.08 (11H, m, cyclohexyl protons), 5.52 (1H, s, pyrimidine-H$_5$),

7.26-7.91 (10H, m, Ar-H), 8.35 (1H, s, pyrazole-H_5), 9.53 (1H, s, NH, D_2O exchangeable); ^{13}C NMR (DMSO-d_6): δ 25.98, 26.34, 30.75, 30.93, 47.50 (cyclohexyl C), 95.71 (pyrimidinyl C5), 175.20 (CS), 104.60, 112.00, 119.07, 121.74, 123.77, 125.18, 126.58, 127.40, 128.59, 128.73, 130.23, 139.62, 141.00, 141.25, 150.07, 154.69 (arom. C); MS, m/z (%): 453 [M^++1] (25), 454 [M^++2] (20), 55 [C_4H_7] (100); Anal. For $C_{27}H_{24}N_4OS$ (452.57): Calcd. C, 71.65; H, 5.35; N, 12.38; S, 7.09; Found: C, 71.51; H, 5.16; N, 12.57; S, 7.22.

4.1.5.3. 6-(3-(Benzofuran-2-yl)-1-phenyl-1H-pyrazol-4-yl)-4-(1H-pyrrol-2-yl)pyrimidine-2(1H)-thione (6c)

Yield 79%, mp. 138-140^{o}C, yellowish brown powder; IR (KBr, cm^{-1}): 3249, 3126 (2NH), 3059 (CH-arom.), 1254 (CS); ^1H NMR (DMSO-d_6): δ 5.02 (1H, s, pyrimidine-H_5), 7.20-7.91 (13H, m, Ar-H, pyrrole protons), 8.50 (1H, s, pyrazole-H_5), 9.20 (1H, s, NH, D_2O exchangeable); ^{13}C NMR (DMSO-d_6): δ 98.54 (pyrimidinyl C5), 177.87 (CS), 104.23, 110.35, 111.67, 111.91, 112.53, 119.34, 121.28, 122.61, 123.05, 123.78, 124.32, 124.90, 125.49, 126.95, 128.72, 131.10, 140.27, 141.54, 149.25, 151.61, 155.28 (arom. C) ; MS, m/z (%): 435 [M^+] (41), 393 [M^++1] (35), 80 [C_5H_6N] (100); Anal. For $C_{25}H_{17}N_5OS$ (435.50): Calcd. C, 68.95; H, 3.93; N, 16.08; S, 7.36; Found: C, 68.74; H, 3.74; N, 16.26; S, 7.54.

4.1.5.4. 6-(3-(Benzofuran-2-yl)-1-phenyl-1H-pyrazol-4-yl)-4-(furan-2-yl)pyrimidine-2(1H)-thione (6d)

Yield 71%, mp. 192-194^{o}C, brown powder; IR (KBr, cm^{-1}): 3127 (NH), 3053 (CH-arom.), 1250 (CS); ^1H NMR (DMSO-d_6): δ 5.51 (1H, s, pyrimidine-H_5), 6.53, 6.66 (2H, m, furan protons),7.31-7.93 (11H, m, Ar-H, furan proton), 8.45 (1H, s, pyrazole-H_5), 9.15 (1H, s, NH, D_2O exchangeable); ^{13}C NMR (DMSO-d_6): δ 96.58 (pyrimidinyl C5), 175.66 (CS), 105.21, 111.66, 112.51, 118.82, 119.24, 121.65, 123.72, 124.38, 125.53, 126.94, 128.40, 130.59, 140.02, 141.34, 145.70, 146.08, 150.61, 155.27 (arom. C); MS, m/z (%): 436 [M^+] (10), 403 [M^+-SH] (12), 77 [C_6H_5] (100); Anal. For $C_{25}H_{16}N_4O_2S$ (436.49): Calcd. C, 68.79; H, 3.69; N, 12.84; S, 7.35; Found: C, 68.56; H, 3.80; N, 12.62; S, 7.18.

4.2. Pharmacology

4.2.1. Evaluation of cytotoxic activity against a panel of sixty human cancer cell lines

The selected compounds by NCI were evaluated for their anticancer activity in a two-stage process. First, these compounds were screened against the full NCI 60 cell lines panel representing leukemia, Non-Small Cell Lung Cancer, melanoma, colon cancer, CNS cancer, breast cancer, ovarian cancer, renal cancer and prostate cancer at a single high dose of 10^{-5} M. Then, the output from the single dose screen is reported as a mean graph and is available for analysis by the COMPARE program. Second, compounds exhibiting significant growth inhibition were evaluated against the 60 cell panel at five different minimal concentrations (0.01, 0.1, 1, 10 and 100 µM).

a. Assay protocol

The human tumor cell lines of the cancer-screening panel are grown in RPMI 1640 medium containing 5% fetal bovine serum and 2 mM L-glutamine. For a typical screening experiment, cells are inoculated into 96 well microtiter plates in 100 mL at plating densities ranging from 5000 to 40,000 cells/well depending on the doubling time of individual cell lines. After cell inoculation, the microtiter plates are incubated at 37^{o}C, 5% CO_2, 95% air and 100% relative humidity for 24h prior to addition of the experimental drugs. After 24h, two plates of each cell line are fixed in situ with TCA, to represent a measurement of the cell population for each cell line at the time of drug addition (Tz). The experimental drugs are solubilized in dimethyl sulfoxide at 400-fold the desired final maximum test concentration and stored frozen prior to use. At the time of drug addition, an aliquot of frozen concentrate is thawed and diluted to twice the desired final maximum test concentration with complete medium containing 50 mg/mL Gentamicin. Additional four, 10-fold or ½ log serial dilutions are made to provide a total of five drug concentrations plus control. Aliquots of 100 mL of these different drug dilutions are added to the appropriate microtiter wells already containing 100 mL of medium, resulting in the required final drug concentrations. Following drug addition, the plates are incubated for an additional 48 h at 37^{o}C, 5% CO_2, 95% air, and 100% relative humidity. For adherent cells, the assay is terminated by the addition of cold TCA. Cells are fixed in situ by the gentle addition of 50 ml of cold 50% (w/v) TCA (final concentration, 10% TCA) and incubated for 60 min at 4^{o}C. The supernatant is discarded, and the plates are washed five times with tap water and air dried. Sulforhodamine B (SRB) solution (100 mL) at 0.4% (w/v) in 1% acetic acid is added to each well, and plates are incubated for 10 min at room temperature.

After staining, unbound dye is removed by washing five times with 1% acetic acid and the plates are air dried. Bound stain is subsequently solubilized with 10 mM trizma base, and the absorbance is read on an automated plate reader at a wavelength of 515 nm. For suspension cells, the methodology is the same except that the assay is terminated by fixing settled cells at the bottom of the wells by gently adding 50 ml of 80% TCA (final concentration, 16% TCA).

b. Data analysis

Using the seven absorbance measurements [time zero, (Tz), control growth, (C), and test growth in the presence of drug at the five concentration levels (Ti)], the percentage growth is calculated at each of the drug concentrations levels. Percentage growth inhibition is calculated as: [(Ti-Tz)/(C-Tz)] × 100 for concentrations for which Ti ≥ Tz and [(Ti-Tz)/Tz] ×100 for concentrations for which Ti < Tz: three dose response parameters are calculated for each experimental agent. Growth inhibition of 50% (GI_{50}) is calculated from [(Ti-Tz)/(C-Tz)] ×100 = 50, which is the drug concentration resulting in a 50% reduction in the net protein increase (as measured by SRB staining) in control cells during the drug incubation. The drug concentration resulting in total growth inhibition (TGI) is calculated from Ti ¼ Tz. The LC_{50} (concentration of drug resulting in a 50% reduction in the measured protein at the end of the drug treatment as compared to that at the beginning) indicating a net loss of cells following treatment is calculated from [(Ti-Tz)/Tz] ×100 = -50. Values are calculated for each of these three parameters if the level of activity is reached; however, if the effect is not reached or is exceeded, the value for that parameter is expressed as greater or less than the maximum or minimum concentration tested [32,33]. Results for each compound were reported as a mean graph of the percent growth of the treated cells when compared to the untreated control cells. There after obtaining the results for one dose assay, analysis of historical Development Therapeutics Programme (DTP) was performed and compounds which satisfies predetermined threshold inhibition criteria is selected for NCI full panel 5 dose assay.

4.2.2. In-vitro enzyme inhibition assay

The profiling evaluation of *in-vitro* Src kinase inhibition by compound **4c** was carried out in Kinexus Corporation, Vancouver, BC, Canada using radiolabeled ^{33}P-ATP assay format. The assay condition for the protein kinases was optimized to yield acceptable enzymatic activity. A radioisotope assay format was used for profiling evaluation of protein kinase target and all assays are performed in a designated

radioactive working area. Protein kinase assays (in singlicate) were performed at ambient temperature for 20-30 minutes in a final volume of 25 µL according to the following assay reaction recipe: 5 µL of diluted active protein kinase (~10-50 nM final concentration in the assay), 5 µL of stock solution of substrate, 5 µL of kinase assay buffer, 5 µL of compound (50 µM) or 10% DMSO, 5 µL of 33P-ATP (250 µM stock solution, 0.8 µCi). The assay was initiated by the addition of 33P-ATP and the reaction mixture incubated at ambient temperature for 20-30 minutes. After the incubation period, the assay was terminated by spotting 10 µL of the reaction mixture onto a Multiscreen phosphocellulose P81 plate. The Multiscreen phosphocellulose P81 plate was washed 3 times for approximately 15 minutes each in a 1% phosphoric acid solution. The radioactivity on the P81 plate was counted in the presence of scintillation fluid in a Trilux scintillation counter. Blank control was set up that included all the assay components except the addition of the appropriate substrate (replaced with equal volume of assay dilution buffer). The corrected activity for protein kinase target was determined by removing the blank control value.

4.3. Docking studies

4.3.1. Target preparation

The crystal structure of Src ATP kinase in complex with AP23451 was retrieved from the RCSB Protein Data Bank (PDB ID: 2BDF) http://www.rcsb.org and was used as a target for our modelling studies. All water molecules were deleted, hydrogen atoms were added and energy of the system was minimized with MOE 2008.10.

4.3.2. Ligand preparation

Compound **4c** was prepared with MOE 2008.10 (Molecular Operating Environment (http: //www.chemcomp.com.). Ligand structure was built with MOE and the energy was minimized using the MMFF94x force field until RMSD gradient of 0.05 Kcal mol^{-1} Å -1 was reached.

4.3.3. Molecular Docking

Co-crystalized ligand and compound **4c** were docked with MOE 2008.10[27] within the pocket sites of the target kinases. The site of docking was considered using crystallographic ligand position. The second step of the procedure was Placement that

was chosen to be Triangle Matcher. The third step was Rescoring 1 which was set to be London dG. Refinement step was chosen to be Force field. The last step: Rescoring 2 was selected to be Affinity dG.

Acknowledgments

This work was supported financially by National Research Centre fund under project No. P 90202. Also, the authors are thankful to the National Cancer Institute (NCI), Bethesda, Maryland, USA, for performing the anticancer evaluation over the 60-cancer cell line panel.

References

[1]. P.P. Kattimani, R.R. Kamble, M.Y. Kariduraganavar, A. Dorababu, R.K. Hunnur, Eur J Med Chem 62 (2013) 232-240.

[2]. T. Nasr, S. Bondock, M. Youns, Eur J Med Chem 76 (2014) 539-548.

[3]. I. Hayakawa, R. Shioya, T. Agatsuma, H. Furukawab, Y. Suganoa, Bioorg. Med. Chem. Lett. 14 (2004) 3411-3414.

[4]. I. Pevet, C. Brulé, A. Tizot, A. Gohier, F. Cruzalegui, J.A. Boutin, S. Goldstein, Bioorg. Med. Chem. 19 (2011) 2517-2528.

[5]. K. Parang, G. Sun, Expert Opin. Ther. Patents 15(9) (2005) 1183-1207.

[6]. K.M. Kasiotis, E.N. Tzanetou, S.A. Haroutounian, fchemistry 2 (2014) 1-7.

[7]. J.M. Summy, G.E. Gallick, Cancer Metastasis Rev. 22 (2003) 337-358.

[8]. T.J. Yeatman, Nat. Rev. Cancer 4 (2004) 470-480.

[9]. B. Boyer, A.M. Valles, N. Edme, Biochem. Pharmacol. 60 (2000) 1091-1099.

[10]. M.C. Frame, Biochim. Biophys. Acta 1602 (2002) 114-130.

[11]. D. Shalloway, P.M. Coussens, P. Yaciuk, Proc. Natl. Acad. Sci. USA. 81 (1984) 7071-7075.

[12]. O. Tatorov, T.J. Mitchell, M. Seywright, H.Y. Leung, V.G. Brunton, J. Edwards, Clinical Cancer Research 15 (2009) 3540-3549.

[13]. A.K.M. Hasan, I. Takashi, S. Ken-ichi, Journal of Signal Transduction 2012 (2012), http://dx.doi.org/10.1155/2012/483796.

[14]. A.S. Tsao, D. He, B. Saigal, S. Liu, J.J. Lee, S. Bakkannagari, N.G. Ordonez, W.G. Hong, I. Wistuba, F.M. Johnson, Cancer Ther. 6 (2007) 1962-1972.

[15]. D.M. Berger, M. Dutia, G. Birnberg, D. Powell, D.H. Boschelli, Y.D. Wang, M. Ravi, D. Yaczko, J. Golas, J. Lucas, F.J. Boschelli, Med. Chem. 48 (2005) 5909-5920.

[16]. S. Khanage, P. Mohite, R. Pandhare, A. Raju, Marmara Pharmaceutical Journal 16 (2012) 134-140.

[17]. K. Ajay Kumar, P. Jayaroopa, IJPCBS 3(2) (2013) 294.

[18]. P. Indovina, F. Giorgi, V. Rizzo, B. Khadang, S. Schenone, D. Di Marzo, I.M. Forte, Oncogene 286 (2011) 1-10.

[19]. S. Dincer, K. Taylan Cetin, A. Onay-Besikci, S. Ölgen, J. Enzym. Inhib. Med Chem. 28(5) (2013) 1080-1087.

[20]. M.I. El-Zahar, S.S. Abd El-Karim, M.M. Anwar, S. Afr. J. Chem. 62 (2009) 189-199.

[21]. M.D. Altıntop, A. Ozdemir, G. Turan-Zitouni, S. Ilgın, O. Atlı, R. Demirel, Z.A. Kaplancıklı, Eur. J. Med Chem., 92 (2015) 342-352.

[22]. A. Solankee, K. Kapadia, A. Ciric, M. Sokovic, I. Doytchinova, A. Geronikaki, Eur. J. Med. Chem. 45 (2010) 510-518.

[23]. N.B. Patel, H.R. Patel, ARKIVOC, xii (2009) 302-321.

[24]. R.H. Shoemaker, Nat. Rev. Cancer 6 (2006) 813-823.

[25]. I. Rubelj, V. Stepanić, D. Jelić, N.S. Vidaček, A.Ć. Kalajžić, M. Ivanković, K. Nujić, M. Matijašić, D. Verbanac, Molecules 17 (2012) 7864-7886.

[26]. S. Gobessi, L. Laurenti, P.G. Longo, S. Sica, G. Leone, D.G. Efremov, Blood 109 (2007) 2032-2039.

[27]. J.E. Castro, C.E. Prada, O. Loria, A. Kamal, L. Chen, F.J. Burrows, T.J. Kipps, blood 106 (7) (2005) 2506-2512.

[28]. Molecular Operating Environment (http://www.chemcomp.com.).

[29]. D. Dalgarno, T. Stehle, P. Narula, P. Schelling, Chem. Biol. Drug Des. 67 (2006) 46-57.

[30]. C.A. Lipinski, F. Lombardo, B.W. Dominy, P. Feeney, J Adv. Drug Deliv. Rev. 46 (3) (2001) 3-26.

[31]. K. Palm, P. Stenberg, K. Luthman, P. Artursson, Pharm. Res. 14 (1997) 568-571.

[32]. M.C. Alley, D.A. Scudiero, A. Monks, M.L. Hursey, M.J. Czerwinski, D. L. Fine, B. J. Abbott, J.G. Mayo, R.H. Shoemaker, M.R. Boyd, Cancer Res. 48 (1988) 589-601

[33]. M.R. Grever, S.A. Schepartz, B.A. Chabner, The National Cancer Institute: cancer drug discovery and development program, Semin. Oncol. 19 (1992) 622-638.

Figure captions:

Fig. 1: Examples of 2-substituted-benzofurans and *N*-substituted pyrazoles as Src protein tyrosine kinase inhibitors

Fig. 2: Design of benzofuran-pyrazole derivatives as Src inhibitors.

Fig. 3: The docked co-crystalized ligand (yellow, stick) showed the same binding mode of native ligand (green, stick). The protein represented as cartoon (light magenta). The important amino acids involved in the interaction (grey, stick).

Fig. 4: The interaction of compound **4c** (magenta, stick) within Src ATP binding site. NH of pyrrole moiety formed H-bond with Lys 343 (2.78Å), N of pyrazoline moiety formed H-bond with Ser345 (3.24Å). Phenyl group of benzofuran moiety was surrounded on by Tyr340, Met341and Ser342.

Fig. 5: Compound **4c** (magenta, stick) and native ligand (green, stick) within Src ATP showed the same binding mode indicating good fitting of compound **4c** within the pocket site.

Fig. 6: Structure activity relationship (SAR) of benzofuran-pyrazole derivatives as anticancer agents.

Scheme caption:

Scheme 1: Synthesis of chalcone, pyrazoline, isoxazole and thiopyrimidine derivatives.

Table captions:

Table 1: Anticancer screening results of eight selected target compounds against sixty human tumor cell lines at single dose assay (10^{-5} M concentration); data was presented as cell growth promotion percentage.

Table 2: NCI *in vitro* testing results of compound **4c** at five different dose levels in μM.

Table 3: Enzyme inhibition assay of compound **4c** against eight different tyrosine kinases.

Table 4: Calculated Lipinskiís rule of compound **4c** within Src ATP Kinase.

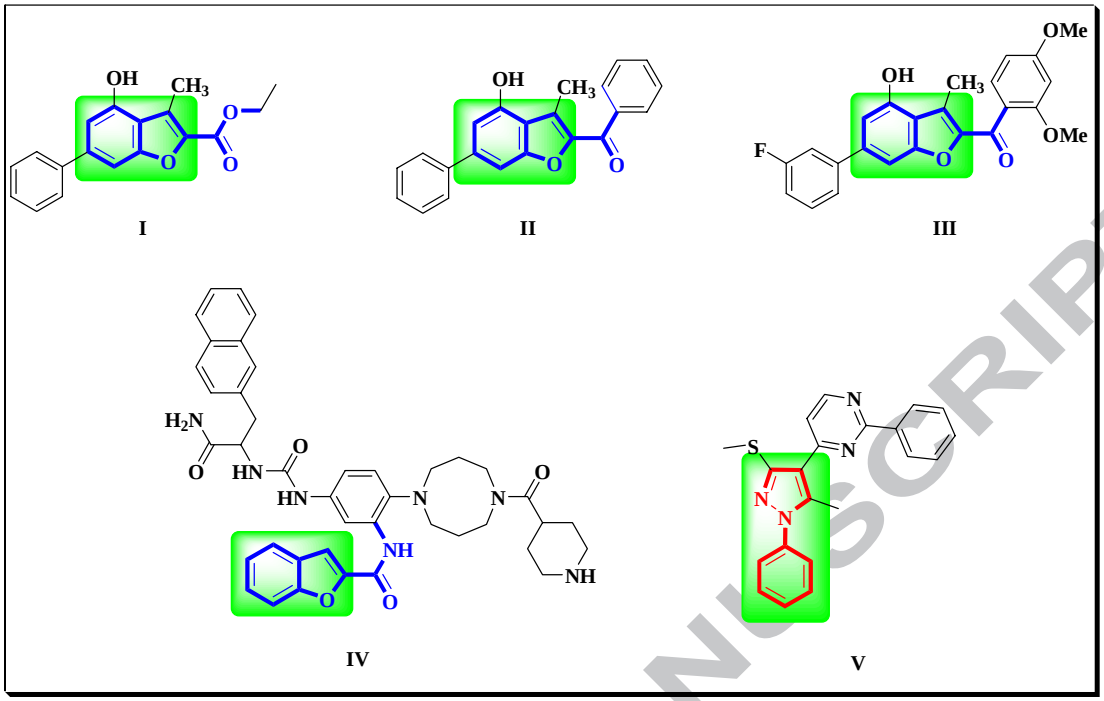

Fig. 1: Examples of 2-substituted-benzofurans and *N*-substituted pyrazoles as Src protein tyrosine kinase inhibitors

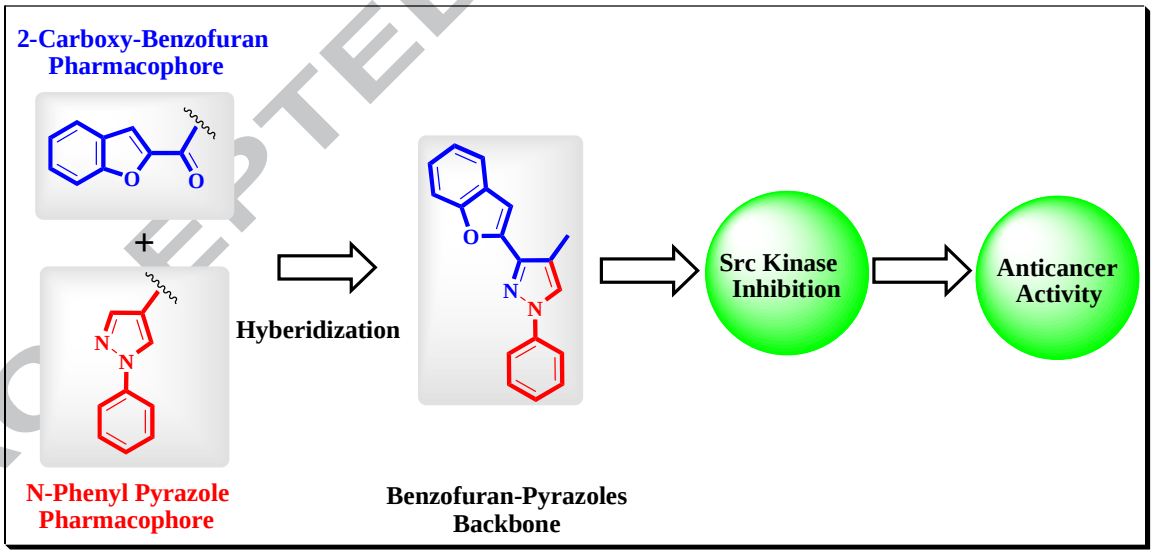

Fig. 2: Design of benzofuran-pyrazole derivatives as c-Src inhibitors.

Fig. 3: The docked co-crystalized ligand (yellow, stick) showed the same binding mode of native ligand (green, stick). The protein represented as cartoon (grey). The important amino acids involved in the interaction (grey, stick).

Fig. 4: The interaction of compound **4c** (magenta, stick) within Src ATP binding site. NH of pyrrole moiety formed H-bond with Lys 343 (2.78Å), N of the pyrazoline moiety formed H-bond with Ser345 (3.24Å). The phenyl group of benzofuran moiety was surrounded by Tyr340, Met341and Ser342.

Fig. 5: Compound **4c** (magenta, stick) and native ligand (green, stick) within Src ATP showed the same binding mode indicating good fitting of compound **4c** within the pocket site.

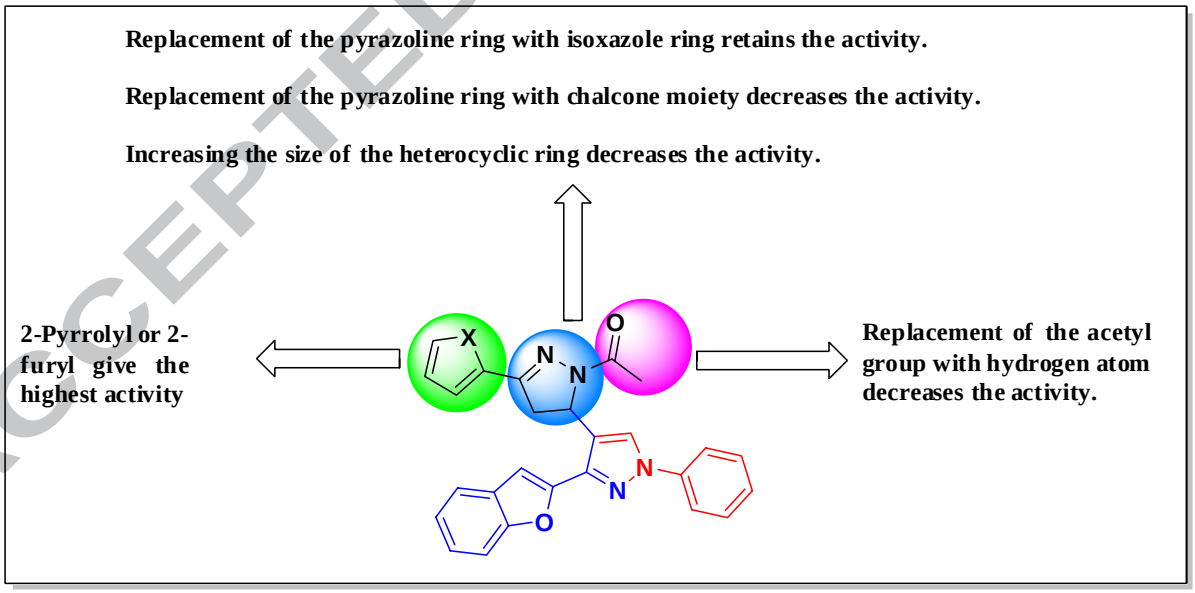

Fig. 6: Structure activity relationship (SAR) of benzofuran-pyrazole derivatives as anticancer agents.

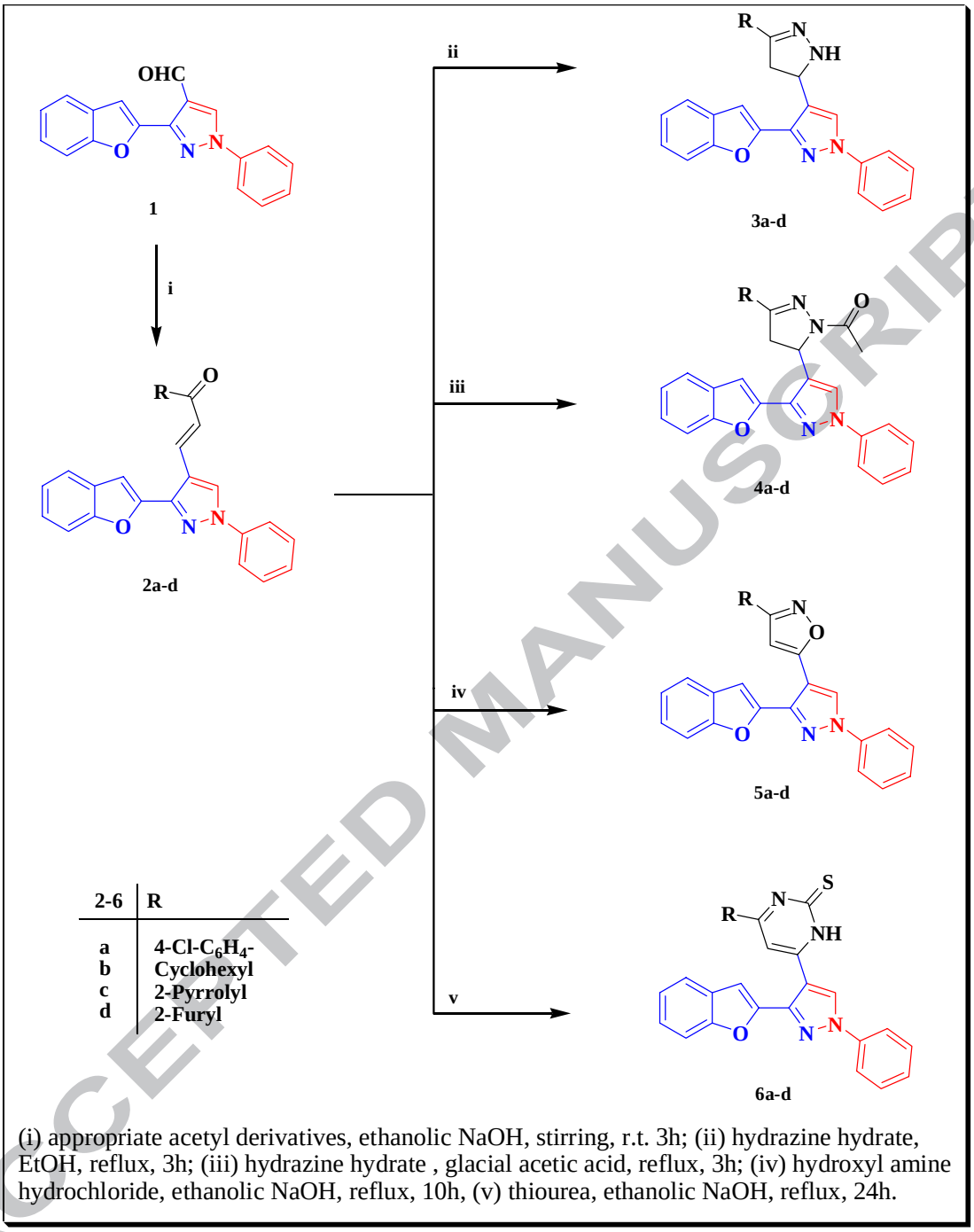

Scheme 1: Synthesis of chalcone, pyrazoline, isoxazole and thiopyrimidine derivatives.

Graphical abstract

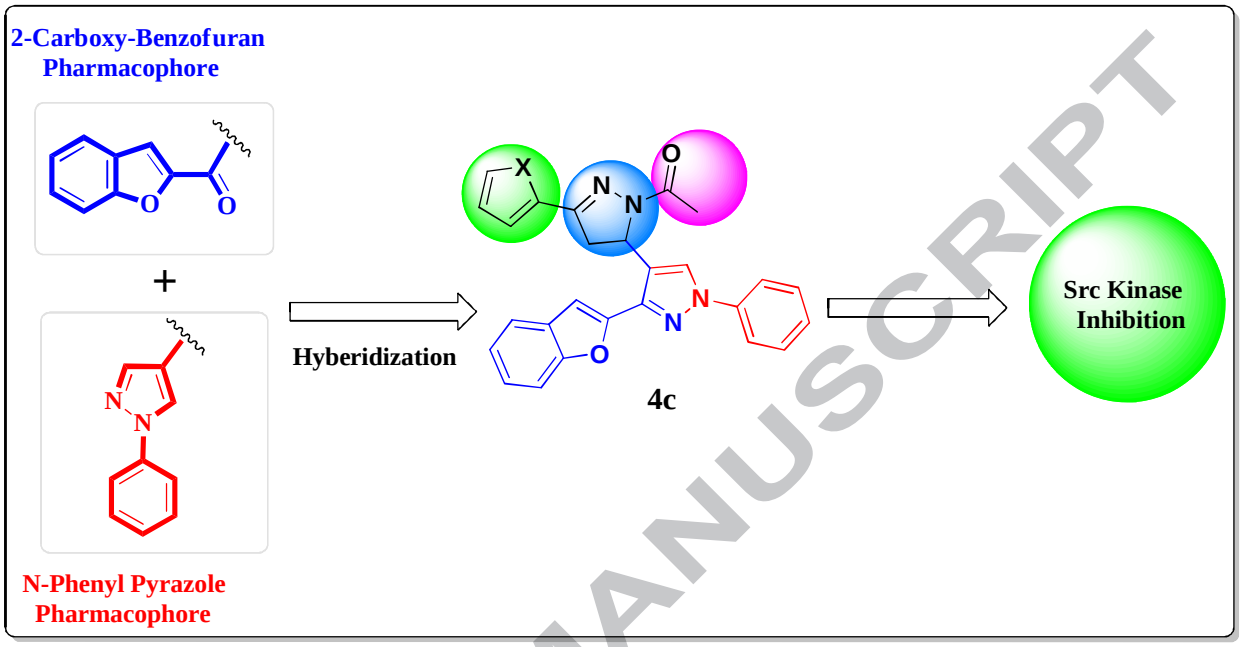

Table 1: Anticancer screening results of eight selected target compounds against sixty human tumor cell lines at single dose assay (10^{-5} M concentration); data was presented as cell growth promotion percentage.

Panel	Subpanel	2c	2d	3c	4c	4d	5d
Leukemia	CCRF-CEM	72.41	98.80	84.53	90.65	78.58	57.57
	HL-60 (TB)	92.07	NA[a]	NA	NA	NA	NA
	K-562	74.02	NA	NA	43.16	88.01	82.64
	MOLT-4	69.07	67.04	74.85	72.32	21.91	50.54
	RPMI-8226	92.87	NA	93.01	62.85	83.09	85.51
	SR	67.66	75.95	85.82	39.11	68.12	44.22
Non-small cell lung cancer	A549/ATCC	85.07	98.71	91.39	62.56	93.67	71.17
	HOP-62	90.87	94.87	NA	74.44	96.60	83.36
	HOP-226	75.00	73.07	87.99	NT[b]	NT	76.41
	NCI-H226	81.04	84.60	87.72	56.25	68.35	71.15
	NCI-H23	87.19	98.83	NA	69.92	74.60	92.15
	NCI-H322M	NA	NA	NA	59.13	NA	98.00
	NCI-H460	90.71	NA	96.41	19.08	97.14	84.31
	NCI-H522	76.82	83.35	86.28	63.39	76.17	67.49
Colon Cancer	COLO 205	NA	NA	NA	87.03	NA	97.65
	HCC-2998	NA	NA	NA	91.87	NA	NA
	HCT-116	71.45	90.38	93.49	27.86	74.80	66.09
	HCT-15	75.14	95.66	93.12	81.86	88.62	78.77
	HT29	92.82	NA	NA	70.07	94.67	NA
	KM12	76.28	93.68	NA	58.51	89.41	80.08
	SW-620	NA	NA	NA	59.18	85.53	NA
CNS Cancer	SF-268	93.44	81.69	93.79	61.23	89.57	69.44
	SF-295	91.79	NA	NT	61.50	91.98	89.12

	SF-539	92.23	95.83	NA	62.41	88.55	91.78
	SNB-19	NA	97.69	NA	NA	85.41	81.05
	SNB-75	72.53	80.43	79.83	41.98	75.47	55.60
	U251	92.51	94.35	89.35	26.06	82.94	77.92
Melanoma	LOX IMVI	79.27	88.93	96.06	27.31	91.32	84.57
	MALME-3M	NA	90.57	93.56	-2.87	74.33	98.04
	M14	87.64	91.60	96.19	75.45	88.50	74.82
	MDA-MB-435	97.24	NA	NA	49.54	81.64	87.50
	SK-MEL-2	87.73	90.82	NA	84.55	72.94	78.63
	SK-MEL-28	97.61	NA	NA	68.69	NA	98.77
	SK-MEL-5	89.99	95.49	94.94	79.26	26.70	89.69
	UACC-257	NA	NA	NA	86.97	79.51	90.65
	UACC-62	84.58	80.32	96.38	76.94	59.63	70.20
Ovarian Cancer	IGROV1	92.10	86.02	94.73	73.59	76.46	75.75
	OVCAR-4	NA	97.02	NA	43.55	62.50	86.01
	OVCAR-5	96.62	98.18	NA	97.03	99.55	99.67
	OVCAR-8	79.08	98.59	NA	55.50	93.54	89.59
	NCI/ADR-RES	84.79	94.52	NA	73.30	89.77	86.90
	SK-OV-3	NA	NA	NA	90.43	88.14	NA
Renal Cancer	786-0	90.66	NA	NA	-38.80	90.92	96.50
	A498	NA	NA	NA	57.71	93.41	NA
	ACHN	81.65	90.73	NA	43.85	82.36	78.52
	CAKI-1	80.48	77.84	NT	63.46	83.51	62.13
	RXF 393	90.95	93.08	85.17	51.49	77.37	NA
	SN12C	88.45	98.13	NA	76.76	88.93	79.79
	TK-10	NA	NA	NA	26.36	NA	NA
	UO-31	71.41	59.33	83.08	65.82	67.00	65.76
Prostate Cancer	PC-3	82.99	84.17	86.80	42.71	58.63	56.34

	DU-145	97.66	95.50	NA	63.30	NA	96.69
Breast Cancer	MCF7	50.98	73.23	74.87	55.44	58.28	51.64
	MDA-MB-231/ATCC	81.89	81.05	96.10	51.24	70.96	55.64
	HS 578T	88.24	94.03	NA	45.95	92.67	93.78
	BT-549	80.02	89.34	NA	78.75	92.52	88.94
	T-47D	55.66	92.35	71.99	54.47	62.95	45.28
	MDA-MB-468	91.52	NA	NA	78.63	22.28	87.77
[a]NA: No activity, [b]NT: Not tested							

Table 2: NCI *in vitro* testing results of compound 4c at five different dose levels in µM.

Panel	Subpanel	GI_{50}	MG-MID[a]	TGI	LD_{50}
Leukemia	CCRF-CEM	1.00	2.63	> 1.00	> 1.00
	HL-60 (TB)	7.98		> 1.00	> 1.00
	MOLT-4	1.00		> 1.00	> 1.00
	RPMI-8226	DNS[b]		> 1.00	> 1.00
	SR	3.17		> 1.00	> 1.00
Non-Small Cell Lung Cancer	A549/ATCC	4.96	5.56	> 1.00	>1.00
	HOP-62	6.54		5.70	> 1.00
	HOP-92	2.15		8.06	> 1.00
	NCI-H226	7.17		7.76	> 1.00
	NCI-H23	5.50		> 1.00	> 1.00
	NCI-H322M	8.64		> 1.00	> 1.00
	NCI-H460	5.55		> 1.00	> 1.00
	NCI-H522	4.02		> 1.00	> 1.00
Colon Cancer	COLO 205	4.40	5.10	> 1.00	> 1.00

	HCC-2998	2.71		> 1.00	> 1.00
	HCT-116	3.16		> 1.00	> 1.00
	HCT-15	4.43		> 1.00	> 1.00
	KM12	9.53		> 1.00	> 1.00
	SW-620	6.39		> 1.00	> 1.00
CNS Cancer	SF-268	7.05	5.20	> 1.00	> 1.00
	SF-295	4.42		> 1.00	> 1.00
	SF-539	3.18		2.66	>1.00
	SNB-19	8.35		> 1.00	> 1.00
	SNB-75	1.79		7.17	> 1.00
	U251	6.41		> 1.00	> 1.00
Melanoma	LOX IMVI	7.04	4.38	> 1.00	> 1.00
	M14	5.56		> 1.00	> 1.00
	MDA-MB-435	5.98		> 1.00	> 1.00
	SK-MEL-2	2.57		> 1.00	> 1.00
	SK-MEL-28	2.85		> 1.00	> 1.00
	SK-MEL-5	2.80		1.80	> 1.00
	UACC-257	5.00		> 1.00	> 1.00
	UACC-62	3.13		> 1.00	> 1.00
Ovarian Cancer	IGROV1	1.90	5.00	> 1.00	> 1.00
	OVCAR-3	6.48		> 1.00	> 1.00
	OVCAR-4	3.97		8.49	> 1.00
	OVCAR-5	DNS		> 1.00	> 1.00
	OVCAR-8	8.86		> 1.00	> 1.00
	NCI/ADR-RES	6.37		> 1.00	> 1.00
	SK-OV-3	7.46		> 1.00	> 1.00
Renal Cancer	786-0	2.54	5.24	7.53	6.78
	A498	4.77		> 1.00	> 1.00

	ACHN	4.01		> 1.00	> 1.00
	CAKI-1	5.98		> 1.00	> 1.00
	RXF 393	2.42		8.36	> 1.00
	SN12C	8.77		> 1.00	> 1.00
	TK-10	6.63		> 1.00	> 1.00
	UO-31	6.81		> 1.00	> 1.00
Prostate Cancer	PC-3	6.67	7.34	> 1.00	> 1.00
	DU-145	8.01		> 1.00	> 1.00
Breast Cancer	MCF7	4.85	3.45	> 1.00	> 1.00
	MDA-MB-231/ATCC	3.50		4.16	> 1.00
	HS 578T	1.26		> 1.00	> 1.00
	BT-549	5.22		> 1.00	> 1.00
	T-47D	2.68		4.59	>1.00
	MDA-MB-468	3.23		> 1.00	> 1.00

[a] MG-MID: Average sensitivity of all cell lines of a particular subpanel towards the test agent in µM.

[b] DNS: Data not shown

Table 3: Enzyme inhibition assay of compound 4c against eight different tyrosine kinases.

.

Target kinase	% Inhibition at 10 µM	
	4c	Staurosprine[a]
SRC	59	83

ZAP70	49	NT[b]
CDK2/Cyclin A2	19	NT
EGFR	8	NT
AURORAA	6	NT
BRA	3	NT
FGFR1	2	NT
PI3Kδ	0	NT

[a] Reference standard used

[b] Not tested

Table 4: Calculated Lipinskiís rule of compound 4c within Src ATP Kinase

Log S	PSA	MW	nH-acc	nH-don	Log p
-6.30	79.42	435.48	1	1	4.30

Log S, solubility parameter; PSA, polar surface area (Å); MW, molecular weight; nH-acc, number of hydrogen bond acceptors; nH-don, number of hydrogen bond donors.

Highlights

- A new series of benzofuran-pyrazole hybrid compounds were designed and synthesized.
- *In In vitro* anti-cancer evaluation against sixty human tumor cell lines.
- *vitro* evaluation of SrcKinase inhibition.
- Molecular modeling in the active sites of Src Kinase.